electronics

MDPI

Article

Machine Learning-Based Satellite Routing for SAGIN IoT Networks

Xueguang Yuan [1], Jinlin Liu [1], Hang Du [1], Yangan Zhang [1], Feisheng Li [2] and Michel Kadoch [3,*]

[1] State Key Laboratory of Information Photonics and Optical Communications, Beijing University of Posts and Telecommunications, Beijing 100876, China; yuanxg@bupt.edu.cn (X.Y.); liujinlin@bupt.edu.cn (J.L.); 7597892@bupt.edu.cn (H.D.); zhang@bupt.edu.cn (Y.Z.)
[2] Department of Applied Mathematics, The Hong Kong Polytechnic University, Hong Kong 999077, China; 21039213r@connect.polyu.hk
[3] Department of Electrical Engineering, ETS, University of Quebec, Montreal, QC H3C 3J7, Canada
* Correspondence: michel.kadoch@etsmtl.ca

Abstract: Due to limited coverage, radio access provided by ground communication systems is not available everywhere on the Earth. It is necessary to develop a new three-dimensional network architecture in a bid to meet various connection requirements. Space–air–ground integrated networks (SAGINs) offer large coverage, but the communication quality of satellites is often compromised by weather conditions. To solve this problem, we propose an extended extreme learning machine (ELM) algorithm in this paper, which can predict the communication attenuation caused by rainy weather to satellite communication links, so as to avoid large path loss caused by bad weather conditions. Firstly, we use Internet of Things (IoT)-enabled sensors to collect weather-related data. Then, the system feeds the data to the extended ELM model to obtain a category prediction for blockage caused by weather. Finally, this information helps the selection of the data transmission link and thus improves the satellite routing performance.

Keywords: space–air–ground integrated network; satellite Internet of Things; limit learning machine model

Citation: Yuan, X.; Liu, J.; Du, H.; Zhang, Y.; Li, F.; Kadoch, M. Machine Learning-Based Satellite Routing for SAGIN IoT Networks. *Electronics* **2022**, *11*, 862. https://doi.org/10.3390/electronics11060862

Academic Editor: Rashid Mehmood

Received: 28 January 2022
Accepted: 7 March 2022
Published: 9 March 2022

1. Space–Air–Ground Integrated Network

1.1. Overview of SAGIN

Space–air–ground integrated networks (SAGIN) include ground networks, satellite systems, and air networks to ensure the reliability and throughput of data transmission [1]. The many combined networks within a SAGIN allow for greater coverage than a traditional ground network [2]. It can provide a secure information infrastructure for sea-, land-, air-, and space-based user activities [3]. In addition, a SAGIN expands the capability of wireless networks, making it an important part of many advanced applications such as autopilot and earth monitoring [4]. There are various complex environments and tasks in future communication. When natural disasters and public emergencies occur, ground communication facilities may be damaged and thus unable meet the needs of communication. SAGINs can achieve fast networking and flexible deployment. At the same time, SAGINs will play an even more important role in the 6G era, appearing as a new trend of future communication networks.

1.2. Architecture for Space–Air–Ground Integrated Network

1.2.1. Introduction of SAGIN Architecture

SAGINs can deal with sophisticated environments in the future, which makes them a developmental tendency in the future communication networks. Figure 1 shows the architecture of a space–air–ground integrated network, it consists of a space network, air network, and ground network, which realizes the sharing of global information and

resources by connecting numerous networks to shape a complicated topology [5]. The specific details of each network are as follows:

(1) Space Network

The space network is made up of various communication satellites distributed in different orbits [6]. Satellite networks can be classified by two indicators: altitude and channel width. Altitude categories include geostationary orbit (GEO), middle-Earth orbit (MEO), and low-Earth orbit (LEO) satellites. Channel width categories include narrowband and broadband. The main advantage of the space layer is that it provides a routing bypass function when direct communication between the space layer and the ground layer is impaired. This bypass function enables the implementation of SAGINs.

(2) Air Network

The air network consists of a variety of aerial communication equipment, such as balloons and unmanned aerial vehicles. The aerial layer has three characteristics: small resource cost, easy deployment, and large coverage [6]. Because of these characteristics, the aerial layer can provide regional wireless access services and routing functions for the ground layer, which make it preferable compared with a base station on the ground.

(3) Ground Network

The ground network consists of users and various ground communication networks including wireless local area networks and cellular networks. The ground layer provides high data rates; however, it fails to service some remote areas.

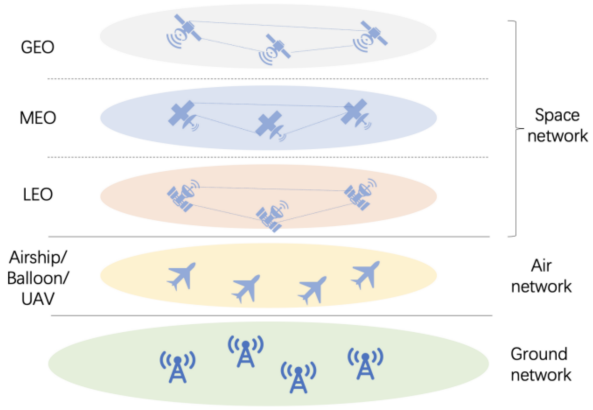

Figure 1. An architecture for a space–air–ground integrated network.

1.2.2. Comparison of Different Networks

Each network layer possesses strengths and weaknesses. The satellite network provides global coverage on the Earth, but there is a long delay in transmission. The ground network has a small propagation delay, so it complements the satellite network. However, the ground network is easily influenced by natural disasters and human factors. Compared with traditional terrestrial networks, SAGINs have an aerial layer so that they have wider coverage, stronger openness, and resistance to various forms of damage [5].

1.2.3. Advantages of SAGIN Architecture

In SAGIN architecture, the three network layers can operate together and work independently. It integrates heterogeneous networks to build a layered broadband wireless network. The satellites may efficiently reach rural and distant regions, significantly lowering the cost of fifth generation (5G) ground networks. Meanwhile, it provides advantages in coverage, throughput, reliability, and flexibility, which provides it with broad application prospects in next-generation networks. In addition, SAGINs are of great importance in many situations such as communication, remote sensing, and navigation.

1.3. Motivation and Main Contributions

An important part of a SAGIN is that the signal transmission between satellites and ground base stations is a kind of wireless signal transmission. These transmissions can be affected by the atmospheric environment. The gas molecules and water vapor condensate in the atmospheric cloud result in electromagnetic wave refraction, reflection, scattering, dispersion, and absorption when propagating. When the cloud thickness is large, it will cause very large signal attenuation. Since the communication path loss between satellites and ground base stations is mainly determined by cloud thickness, rainfall, and the incident angle between the communication link and clouds, the blockage will be calculated according to the above three parameters and divided into six levels for prediction and analysis. Finally, the satellite routing design can be improved according to the predicted blockage, so as to improve the quality of satellite ground communication.

In this article, we propose to use integration of IoT and satellites for weather data collection and transmission. At the same time, we predict communication blockage by an extended ELM model, and therefore find a communication link with the smallest signal loss so that the ground and satellite can communicate through this communication link to improve communication quality. This article connects IoT networks with SAGINs, because satellite connections for IoT networks are well-suited to delivering service where terrestrial networks are absent. Meanwhile, there are many instances where terrestrial coverage exists, but it must cross many different networks, which makes the transmission efficiency very low. SAGINs make it much easier, as they can transmit data from every network. Therefore, by using integration of IoT and satellites for weather data acquisition, transmission, and analysis undoubtedly becomes a more efficient and reliable scheme.

The ELM algorithm has small computational complexity and good overall performance, but it also has some limitations. Because of the simple network model, the ELM algorithm can perform well only for small-scale datasets. Once the data scale increases, the performance of the ELM algorithm will decline sharply. Therefore, we propose an extended ELM model. Based on the original ELM model, several full connection layers are added to the model, so that the model overcomes this limitation, successfully processes large-scale data, and shows good performance. The extended ELM model has a fast calculation speed and high accuracy rate in this scenario. As far as we know, this is the first time that the extended ELM model is embedded in the SAGIN framework to improve the communication efficiency of SAGIN.

2. Architecture Design

2.1. Satellite-Based IoT (SIoT)

2.1.1. Advantages of Satellite Communications

Satellite communications have high accuracy and low delay [7], so they play an important role in the fields of navigation, time service, measurement, and communication. Satellite communications can also provide services in emergency, service delivery, distribution, and the energy Internet, which means satellites have great potential in the future development of IoT networks and next-generation communication networks [8].

2.1.2. Satellite and Ground Communications Complement Each Other

In terrestrial communication systems, it is very difficult to establish ground base stations in poor geographical conditions such as oceans and deserts [7]. As a result, the coverage of terrestrial wireless networks is very limited. Satellite communications, on the other hand, may cover a wide region regardless of geographical constraints and thus can supplement the coverage of terrestrial communication. Nevertheless, the spectrum resources of satellite IoT are limited [9], so satellite IoT needs to share a spectrum with ground IoT which we call 'SIoT'. Satellites can realize communication with high quality and high reliability, which is of great significance to terrestrial communications. By supplementing a network with satellites, it is possible to meet the demand for global coverage. Satellites have become an important and powerful element in the future of communication systems.

2.1.3. Related Works on SIoT

Author Zhicheng Qu mainly introduces the architecture of a LEO satellite constellation for IoT, which contains some access and routing protocols, the structure of a LEO satellite constellation, and compatibility of heterogeneous networks [10]. Author Ahan Kak introduces a satellite IoT based on micro-satellite technology and SDN and the impact of orbital configurations [11].

A satellite-based IoT network is shown in Figure 2. Satellites and IoT are connected by wireless links. The ellipse below represents the satellite coverage area, and there are IoT networks in it. The red dots represent the sensor nodes and the triangular towers represent the IoT trans-receivers. The SIoT network is formed between the satellites and IoT network on the Earth's surface through the above methods.

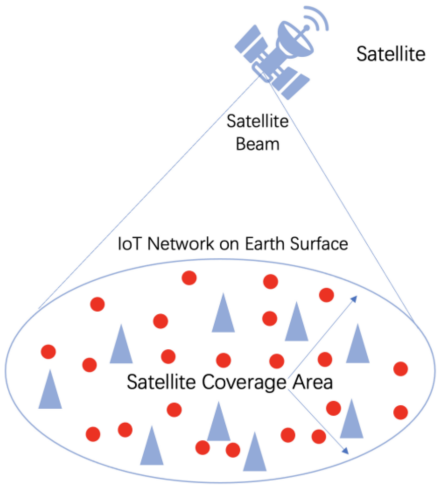

Figure 2. Satellite-based IoT Network.

2.2. Overview of Architecture Design

The perception layer, network layer, and application layer are the three layers that make up the architecture. The perception layer is mainly responsible for collecting data. The network layer, also as the core layer, mainly provides up/down data transmission services. In the satellite network system, the ground node network, satellite backbone network, and satellite access network constitute the satellite network layer. The satellite networks relay sensing data to the core network. For the sake of inter-operation and integration of satellite networks and IoT, it is very significant to establish the terrestrial base stations. In addition, when normal terrestrial terminals are not linked to satellites, we assume that the terrestrial base stations could send the information to the satellites to complete communication between satellites and ground.

Figure 3 shows the schematic diagram of this project. First of all, sensors constitute the main part of perception layer of SIoT, which is responsible for collecting weather data; the IoT network on the Earth's surface and satellite network make up the network layer in SIoT. They mainly provide the up/down data transmission. Satellite routing design belongs to the application layer of SIoT.

The process of the project is as follows: sensors input the collected weather data, such as temperature and humidity, into the extended ELM model. Then, blockage caused by bad weather is derived through classification fitting analysis, applying the extended ELM model. Consequently, the satellite communication routing design can avoid bad weather and improve communication efficiency by adding an extended ELM algorithm to the SAGIN system.

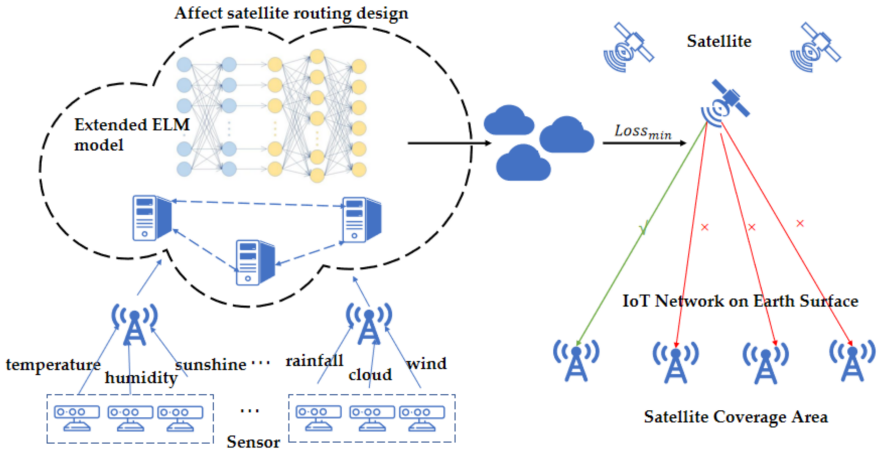

Figure 3. Schematic diagram of the system.

2.3. Perception Layer

The perception layer is composed of IoT devices, such as various sensors. Sensors are used to collect weather-related data, then a connection with the ground base station through IoT is established, and the data could be uploaded to the cloud for analysis. The data collected through the perception layer constitute the dataset of this experiment.

2.4. Network Layer

Figure 4 shows a network model for satellite-based IoT. The network layer is composed of users, a ground segment, and a space segment. In addition, an extended ELM algorithm is added to the network layer, which affects the satellite routing design and improves the communication transmission efficiency of the architecture. Various satellite resources constitute the space segment. The satellites can be categorized as high-orbit satellites and low-orbit satellites.

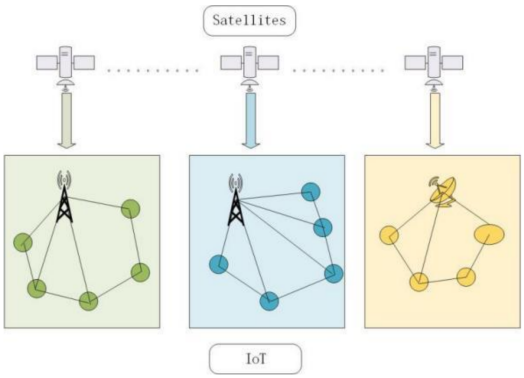

Figure 4. A network model for satellite-based IoT.

(1) High-Orbit Satellite

Inspired by the development of communication services on geosynchronous satellites, high-orbit satellite communication services are studied and derived. A satellite can cover almost half of the globe at high altitudes, which allows it to provide services in an incredibly broad range.

(2) Low-Orbit Satellite

Compared with GEO satellites, a LEO satellite-based IoT has smaller path loss and propagation delay [12]. The LEO satellite-based IoT has the characteristics of high reliability, wide-coverage, and large capacity, thus it is a significant extension of the terrestrial IoT. LEO

satellite communications cannot be affected by ground obstacles, because IoT devices can access the LEO satellites with flexible angles. Furthermore, LEO satellites use multi-beam technology to provide services for more IoT devices.

Consequently, this experiment is based on a LEO satellite-based IoT.

2.5. Application Layer

Satellites play an irreplaceable role in IoT. Smart medicine, smart home, industrial Internet, and other IoT businesses have grown significantly in recent years. Some services need great efficiency over a long length of time and with high dependability. To meet the needs of these services and ensure quality of service, the network has been extended from the ground broadband network to the ground and satellite broadband network. SIoT also plays an important role in some mission-critical applications [13]. The failure of these tasks may lead to significant loss of life and property. For example, in mission-critical military applications, border protection and territorial defense are linked. These applications must successfully protect valuable resources. However, these mission-critical applications present many risks to human life. Therefore, the collection and driving of information should be completed by IoT sensors. The integration of satellites and the Internet of Things improves the coverage and reliability of these mission-critical application networks. At the same time, the wide coverage of SIoT enables application prospects in farms, oil/gas facilities, power grids, etc. [14]. The wide possibilities of SIoT make it an area of particular research interest.

The above mainly introduces the content of satellite routing. It can be seen that, in SAGIN, how to ensure the reliability and effectiveness of satellite communication transmission is very important. Therefore, in the following sections, the method of improving the effective transmission of communication in the SAGIN architecture is mainly introduced, that is, the method proposed to use the extended ELM algorithm to predict the congestion of the communication path.

3. Model Design

3.1. Overall Process of the System

The subject of this paper is the presentation of an analytical model for the prediction of rainfall intensity of the SAGIN system. Figure 5 is the overall process of the system.

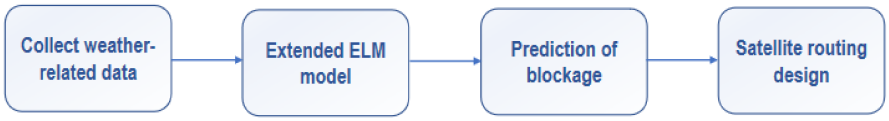

Figure 5. Overall process of the system.

First of all, the system collects weather-related data through IoT sensor devices to form a dataset. Next, the obtained dataset undergoes a series of data preprocessing procedures. The extended ELM model inputs the collected weather-related data, outputs the prediction of blockage which affects the satellite routing design, and improves the reliability and effectiveness of data transmission.

3.2. Influence of Blockage on Satellite Communication Transmission

High-frequency band satellite communication is advantageous due to its small frequency bandwidth equipment and strong anti-interference tendencies. However, high-frequency band satellite communication is greatly affected by the atmospheric environment [15].

At communication frequencies above 10 GHz, rain is the most influential propagation phenomenon on satellite communication links [16]. When the frequency is higher than 20 GHz, heavy rain may cause severe signal attenuation, to the point of interrupt-

ing the communication link. Therefore, this paper focuses on high-frequency satellite communication above 20 GHz.

In all weather conditions, rainfall has the greatest impact on communication congestion, so this paper calculates the communication congestion according to rainfall and other parameters. Based on previous studies on rain attenuation [16], the estimated value of blockage corresponding to different rainfall types can be calculated by Formula (1). Assuming that the frequency band of the satellite is f (Hz), the cloud attenuation corresponding to this frequency band is c (dB/km), the cloud incident angle of satellite communication is a, and the cloud thickness is t, then the blockage of satellite communication in the transmission process can be obtained according to the formula [16]

$$\text{blockage} = \text{t}\ (\text{km}) \times \csc\ (\text{a}^{\circ}) \times \text{c}\ (\text{dB/km}) \quad (1)$$

Table 1 shows the cloud thickness and attenuation corresponding to different levels of rainfall, as well as the blockage in the final satellite communication transmission process obtained from different incident angles. Take heavy rain as an example, assuming that the cloud height is 8 km, the absorption loss of rainfall to radio waves is 20 dB/km, and an antenna elevation angle of 45 degrees, the rain attenuation of frequency band downlink is 226 dB. The table shows that when rainfall increases, the route loss of satellite transmission increases. If the estimation of rain attenuation is not accurate, the design of parameters is unreasonable, which will affect the quality and effectiveness of communication. Therefore, prediction of blockage on communication links is crucial in satellite communication engineering design.

Table 1. Comparison table of blockage caused by bad weather.

	Thickness (km)	**Incident Angle (°)**	**Attenuation (dB/km)**	**Blockage (dB)**
Drizzle	2.5	30	0.2	1
Moderate rain	3	60	3.5	12.1
Heavy rain	8	45	20	226.3

3.3. Denoising with SMOTE Algorithm

The original weather-related data is gathered utilizing sensors and IoT technologies, and that will need a collection of about 140,000 data points. There were approximately 500,000 pieces of data in the dataset after a series of data preprocessing procedures, such as missing value and anomalous value processing, data category imbalance processing, and so on. The dataset includes information such as geographic location, daily minimum and maximum temperatures; as well as temperature, wind speed, humidity, and air pressure at various times of the day, including 9 a.m., 3 a.m., and 3 p.m.

Table 2 shows the data distribution of different rainfall categories in the original data. Among the collected weather data, there is a serious problem of unbalanced data categories. Synthetic minority over-sampling technique (SMOTE) is used to solve this problem. SMOTE is a commonly used over-sampling technique to subside the imbalanced dataset problem [17]. The basic idea of the algorithm is to analyze and simulate minority samples, and add new manually simulated samples to the dataset, so the categories in the original data will not lose balance seriously [18]. At present, the SMOTE algorithm is an excellent way to deal with the imbalanced classification problem.

Table 2. Data distribution and proportion in the original dataset.

	Number	Proportion
No blockage	79,952	64.3%
Micro blockage	35,890	29.0%
Small blockage	5713	4.7%
Intermediate blockage	1832	1.4%
Large blockage	585	0.5%
Huge blockage	138	0.1%

The flow chart of the SMOTE algorithm is shown in Figure 6. First, in a small number of sample sets, for a sample x, the K nearest neighbor samples of x can be obtained by calculating the Euclidean distance from x to other samples [19]. The formula for calculating Euclidean distance is

$$d(x, y) = \sqrt{\sum_{i=1}^{n} (y_i - x_i)^2} \quad (2)$$

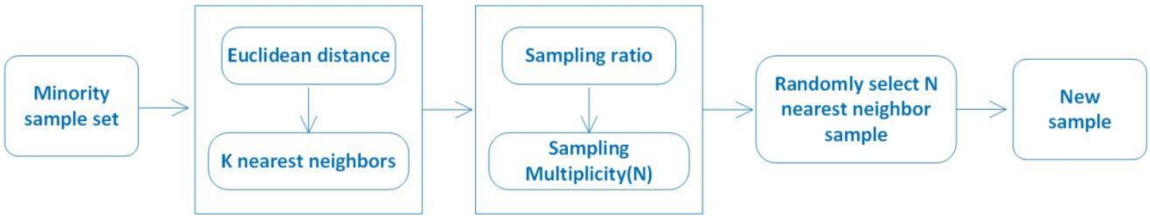

Figure 6. Flow chart of SMOTE algorithm.

Secondly, the sampling rate is set for the samples to obtain the sampling multiplicity, assuming that the sampling multiplicity is represented by n. Then n nearest neighbor samples can be randomly selected from K nearest neighbor samples, and the selected samples are recorded as y [20]. Thirdly, given sample X and sample y, we can construct a new sample set by the formula

$$L = x + \text{rand}(0, 1) \times |x - y| \quad (3)$$

Figure 7 shows the box diagram of 'blockage' data processed by SMOTE algorithm according to category distribution. It can be concluded that the SMOTE algorithm can solve the problem of unbalanced data categories.

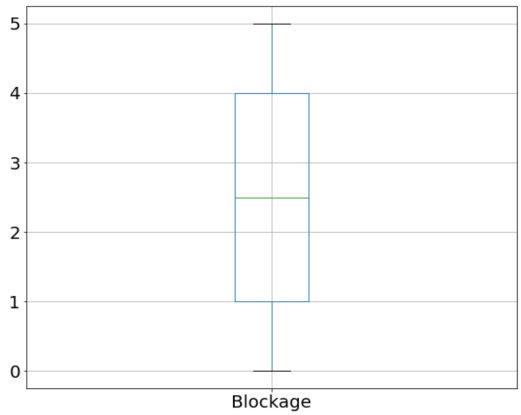

Figure 7. Blockage distribution after data preprocessing using the SMOTE algorithm.

A good-performing classifier may be constructed after rebalancing the class distribution of the training dataset.

3.4. Extended ELM Model Structure Design

The flow chart for the extended ELM model is shown in Figure 8. In the raw data, there will be some missing and null values. These data are first analyzed, then they will be standardized to transform symbol-type data into numbers. Then, the blockage in the communication link is divided into six categories according to its value. To finish the data preparation procedure, the SMOTE algorithm is utilized to process the imbalanced data. Data may be loaded into the ELM model's expanded version. The complete connection layer, which consists of two 128 neural units, is followed by the original ELM model. The ELM model consists of an input layer, a hidden layer in the center, and a six-neuron output layer to output the predicted six blockage categories.

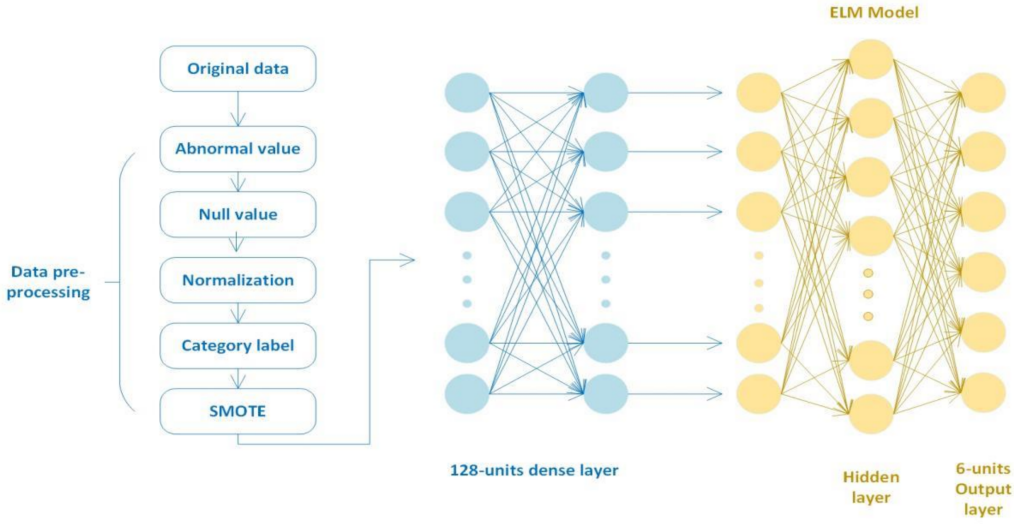

Figure 8. Flow chart of extended ELM model.

The ELM is a single-hidden-layer neural network algorithm, which can be used for the establishment of regression and classification models [21]. Compared with the traditional single hidden layer feed-forward neural network, the input weight and the offset are random. The corresponding output weights are obtained through calculation. Therefore, to ensure learning accuracy, the ELM algorithm has low computational complexity and a good general performance.

Assume that the training sample is represented by $\{(X_i, T_i)\}$, where X_i is the model's input vector and T_i is the model's output vector. The number of neural units in the input layer of the ELM model is N, the number of neural units in the hidden layer is L, and the number of neural units in the output layer is M. The formulas for the ELM model are

$$H\beta = T \tag{4}$$

$$H = \begin{bmatrix} g(\omega_1 \times x_1 + b_1) \cdots g(\omega_L \times x_1 + b_L) \\ g(\omega_1 \times x_2 + b_1) \cdots g(\omega_L \times x_2 + b_L) \\ \vdots \cdots \vdots \\ g(\omega_1 \times x_N + b_1) \cdots g(\omega_L \times x_N + b_L) \end{bmatrix}_{N \times L} \quad \beta = \begin{bmatrix} \beta_1^T \\ \beta_2^T \\ \vdots \\ \beta_L^T \end{bmatrix}_{L \times M} \quad T = \begin{bmatrix} t_1^T \\ t_2^T \\ \vdots \\ t_N^T \end{bmatrix}_{N \times M} \tag{5}$$

$$g(x) = \frac{1}{1 + e^{-x}} \tag{6}$$

The ELM model consists of an input layer, hidden layer, and output layer. ω_i represents the weight between the input layer and β is the hidden layer, b_i is the bias of the hidden layer, and $g(x)$ is the sigmoid function, which is used as the activation function of the neural unit in the hidden layer. Through the activation function, the results of $\omega_i \times x_i + b_i$ mapping form a matrix, which is called the feature mapping matrix H. When the network

is generated, ω_i and b_i will be randomly generated. Then, with the increase in the number of iterations, ω_i and b_i will be gradually adjusted to make the model more accurate. The model combines the matrix H with the vector β multiplication, the resulting matrix as the output of the model, denoted as T.

$$\hat{\beta} = \mathbf{H}^{\dagger}\mathbf{T} \tag{7}$$

The above formula is transformed into the least square solution of the solution $\hat{\beta}$, the Moore–Penrose generalized inverse of matrix H is $H^{\dagger}$.

The Moore–Penrose generalized inverse of matrix H is $H^{\dagger}$. ELM has been widely used in many fields because of its fast training speed, good interpolation ability, and approximation ability.

However, the ELM model also has some problems. When faced with a large-scale, unbalanced, and noisy dataset, its performance is not stable. Therefore, we propose a new model to enhance stability. The network is built using the Python-based open-source artificial neural network framework Keras. The data are input into two full connection layers with 128 nerve units, and the data are pre-trained. Because the data are shuffled after each training, the training and verification sets are resampled. The average accuracy of the model's five training sessions is output, and the k-fold cross-verification technique (5-fold) is used in the training process. The tanh function is used as an activation function in each layer, which can be expressed by the formula

$$f(x) = \frac{e^{x} - e^{-x}}{e^{x} + e^{-x}} \tag{8}$$

Then, the output of the full connection layer is input into the ELM model, the ELM model categorizes the data, and finally the vector classification results are output. The loss function of the model uses categorical cross-entropy, which is used to describe the distance between two distributions. The formula is

$$J = -\sum_{i=1}^{K} y_i \log(p_i) \tag{9}$$

where K is the number of categories, y represents the label, and p is the output of the neural network [22].

In the process of iteration, the root mean square prop (RMSProp) optimization algorithm is used to optimize the model. It has the advantages of small swing amplitude in update and fast convergence speed of loss function. Each formula is as follows:

$$s_{dw} = \beta s_{dw} + (1 - \beta) dW^2 \tag{10}$$

$$s_{db} = \beta s_{db} + (1 - \beta) db^2 \tag{11}$$

$$W = W - \alpha \frac{dW}{\sqrt{s_{dw}} + \varepsilon} \tag{12}$$

$$b = b - \alpha \frac{db}{\sqrt{s_{db}} + \varepsilon} \tag{13}$$

In the above formulas, s_{dw} and s_{db} are the accumulated gradient momentum of the loss function in the previous $(t-1)$ iteration, and β is an index of gradient accumulation. The RMSProp algorithm corrects the swing amplitude by calculating the weighted average value of the square of the gradient differential, which makes the swing amplitude smaller, so the network converges very fast.

The above is the introduction of the algorithm theory and formulas applied in the experimental process. The next section will discuss the simulation results of the extended ELM model in detail.

4. Experimental Simulation Results and Analysis

4.1. Data Analysis

In the process of exploratory data analysis, feature engineering is a very important step. In the process of feature engineering, the characteristics that can better represent the core of the issue and play a greater role in the prediction process will be chosen from the original features. These selected features are put into the model to improve the prediction accuracy and speed of the model. It is necessary to select features that highly correlate with 'blockage' in the dataset to conduct experiments.

The correlation matrix between eigenvalues is shown in Figure 9. It can test the direction and degree of a change trend between any two variables. Covariance is a parameter that measures the magnitude of the mutual influence of two variables. As shown on the right side of Figure 9, the lighter the color in the picture, the larger the correlation coefficient value between the two features, and the darker the color, the smaller the correlation coefficient. The larger the absolute value, the higher the correlation between the two. For this project, there are 21 features and one label. Covariance matrices work well for multidimensional problems like this, and correlations between two features can be seen by looking at the intersection between any two features. Therefore, the degree of correlation between each feature and 'blockage' can be analyzed by looking at the intersection value of 'blockage' and other features.

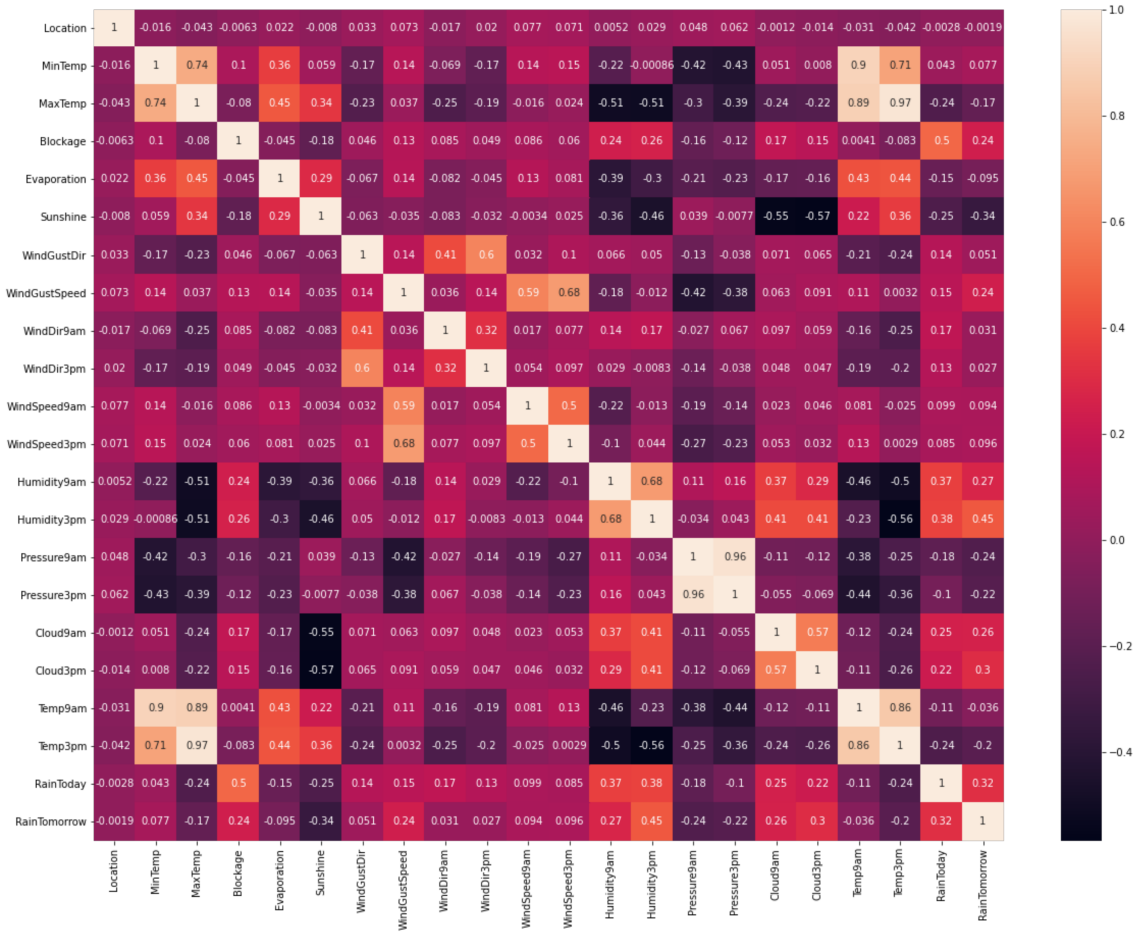

Figure 9. Correlation coefficient between features.

The range of correlation coefficient is −1 to +1. It can be calculated by the formula [20]

$$r_{xy} = \frac{n\sum x_i y_i - \sum x_i \sum y_i}{\sqrt{n\sum x_i^2 - (\sum x_i)^2}\sqrt{n\sum y_i^2 - (\sum y_i)^2}} \tag{14}$$

4.2. Metrics of Extended ELM Model

To characterize the effectiveness of the ELM classification method, the confusion matrix is used to evaluate the performance of the method [23]. The confusion matrix combines accuracy, precision, recall, and F1-score to measure the performance of the classification model. It records the sample number of all classification results in the table. Accuracy, precision, recall, and F1-score are defined as follows:

$$\text{Accuracy} = \frac{TP + TN}{TP + TN + FP + FN} \tag{15}$$

$$\text{Precision} = \frac{TP}{TP + FP} \tag{16}$$

$$\text{Recall} = \frac{TP}{TP + FN} \tag{17}$$

$$F1 - \text{score} = \frac{2TP}{2TP + FP + FN} \tag{18}$$

In the formulas, TP, TN, FP, and FN represent true positive, true negative, false positive, and false negative respectively. In the process of evaluating the model, if only one index of accuracy or recall rate is used, the advantages and disadvantages of the model cannot be fully evaluated. Therefore, the F1 score, as a harmonic average of accuracy and recall rate, can be better used as an evaluation index of model of classification in multi-classification problems.

4.3. Results and Analysis

First, we need to determine the number of neurons. Figure 10 shows the influence of the number of neurons in the hidden layer on the model performance of the extended ELM model. This figure shows the process of analyzing and selecting the number of hidden layer neural units in this experiment, and finding the appropriate value by debugging different numbers of neural units. From left to right, the abscissa indicates the number of concealed layers from 100 to 2000. The value of accuracy, precision, and recall is represented by the ordinate. The graphic shows that, as the number of hidden layers increases, the accuracy, precision, and recall rise, and the model performance improves. When the number of hidden layers is 1500 and more, the performance of the model tends to be stable. To achieve the optimal effect of the model, the final extended ELM model uses 1600 hidden neural units.

The extended ELM model has shown excellent results. Figure 11 shows the confusion matrix of each category. The abscissa represents the prediction category, the ordinate represents the real category, and the sample on the diagonal is the correct prediction sample. The number in the matrix represents the corresponding number of samples. The lower the number of samples, the darker the corresponding color in the matrix and the closer it is to purple. The greater the number of samples, the lighter the corresponding color in the matrix, and the closer it is to yellow. It can be seen from this confusion matrix that most of the sample data is concentrated in the diagonal position of the matrix, therefore, the vast majority of samples were correctly predicted.

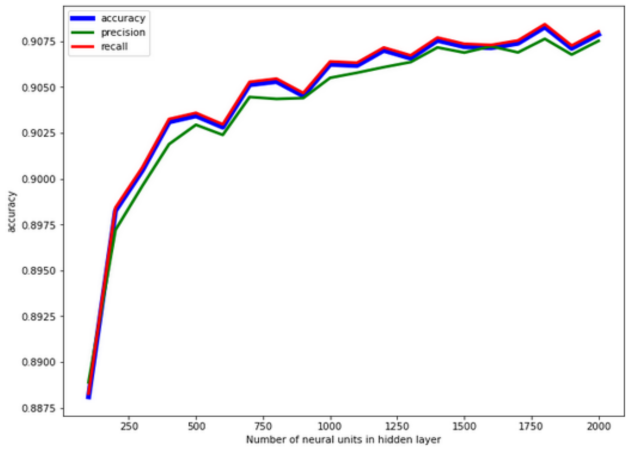

Figure 10. Influence of number of neurons in the hidden layer on the model.

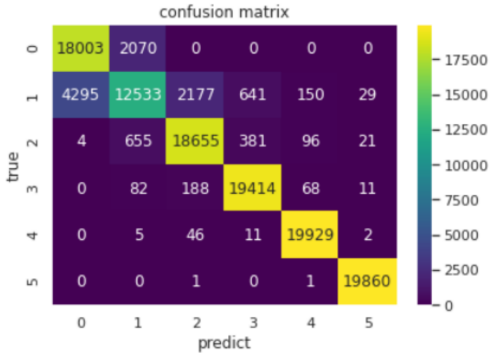

Figure 11. Confusion matrix of testing set.

Table 3 shows the performance of six categories on the four indicators of accuracy—precision, recall, F1-score, and support. Among them, support represents the number of test samples in each category. It can be seen that the classification results obtained by the ELM model are at 91% accuracy.

Table 3. Performance of six categories on each metric.

	Precision	Recall	F1-Score	Support
Class 0	0.81	0.90	0.85	20,073
Class 1	0.82	0.63	0.71	19,825
Class 2	0.89	0.94	0.91	19,812
Class 3	0.95	0.98	0.97	19,763
Class 4	0.98	1.00	0.99	19,993
Class 5	1.00	1.00	1.00	19,862
Accuracy			0.91	119,328
Macro average	0.91	0.91	0.90	119,328
Weighted avg	0.91	0.91	0.90	119,328

Table 4 shows the comparison of the extended ELM model and deep neural network (DNN) model. In terms of the network layers of the model, the extended ELM model has only five layers, so the model is simple. In terms of time consumption, extended ELM consumes less time than DNN, so the model runs very fast. In terms of prediction accuracy, the model accuracy of extended ELM model reaches 91%, so the model is very efficient.

This section introduces the process of model tuning and the performance of the model. Consequently, extended ELM has the advantages of simplicity, fast running speed, and efficiency, as well as having broad development prospects.

Table 4. Time consumed by different models.

	Time (s)	Accuracy (%)	n_Layers
Extended ELM	59.0663	91.0	5
DNN	178.9913	89.1	5

5. Conclusions

The integration of space and ground networks is a good solution with wide coverage and high transmission efficiency. A variety of ELM models are proposed in this paper, to further improve the data transmission quality and improve the stability of data interaction between satellite and ground base station. The blockage predicted by the extended ELM model is one of the most important factors affecting satellite data transmission. The simulation results also show that our model is effective, efficient, and accurate. With the help of the extended ELM model, the satellite can find the data transmission link with the highest transmission efficiency and the fastest transmission speed. This method can not only guarantee data transmission reliability, but also reduce data transfer time and increase data transmission efficiency. The features of the ELM model are its light weight and the ability of the model deployed to many edge devices. Edge devices can quickly and efficiently collect data and fit ELM models locally. The time performance has been greatly improved, further ensuring the stability of the interaction between satellites and ground base stations. Regarding the future development of this work, at present, the model accuracy of this work is limited by the technical limitations of weather collection equipment. If more weather features can be collected in the future, the model performance will be further improved. In addition, rainy weather is not the only influencing factor for the communication efficiency of satellite communication links. In future work, it can be challenged to comprehensively consider multiple influencing factors and propose further optimization schemes for the routing design of the SAGIN architecture.

Author Contributions: Conceptualization and methodology, X.Y.; writing—original draft preparation, writing—review and editing, J.L. and H.D.; software, validation and visualization, Y.Z.; data collection, data analysis and data curation, F.L. and M.K. All authors have read and agreed to the published version of the manuscript.

Funding: This research received no external funding.

Conflicts of Interest: The authors declare no conflict of interest.

References

1. Dai, C.; Li, X.; Chen, Q. Intelligent Coordinated Task Scheduling in Space-Air-Ground Integrated Network. In Proceedings of the 2019 11th International Conference on Wireless Communications and Signal Processing (WCSP), Xi'an, China, 23–25 October 2019; pp. 1–6.
2. Ye, J.; Dang, S.; Shihada, B.; Alouini, M.S. Space-Air-Ground Integrated Networks: Outage Performance Analysis. *IEEE Trans. Wirel. Commun.* **2020**, *19*, 7897–7912. [CrossRef]
3. Yang, Z.; Xiao, B.; Chen, Y. Modeling and Verification of Space-Air-Ground Integrated Networks on Requirement Level Using STeC. In Proceedings of the 2015 International Symposium on Theoretical Aspects of Software Engineering, Nanjing, China, 12–14 September 2015; pp. 131–134.
4. Wang, G.; Zhou, S.; Zhang, S.; Niu, Z.; Shen, X. SFC-Based Service Provisioning for Reconfigurable Space-Air-Ground Integrated Networks. *IEEE J. Sel. Areas Commun.* **2020**, *38*, 1478–1489. [CrossRef]
5. Qu, H.; Luo, Y.; Zhao, J.; Luan, Z. An LBMRE-OLSR Routing Algorithm under the Emergency Scenarios in the Space-Air-Ground Integrated Networks. In Proceedings of the 2020 Information Communication Technologies Conference (ICTC), Nanjing, China, 29–31 May 2020; pp. 103–107.
6. Liu, J.; Shi, Y.; Fadlullah, Z.M.; Kato, N. Space-Air-Ground Integrated Network: A Survey. *IEEE Commun. Surv. Tutor.* **2018**, *20*, 2714–2741. [CrossRef]
7. Shi, Z.; Wu, Z.; Kang, Z.; Chen, X. High and Low Orbit Satellite Mixed Data Transmission System Application for Power Ubiquitous Internet of Things. In Proceedings of the 2019 IEEE 3rd Advanced Information Management, Communicates, Electronic and Automation Control Conference (IMCEC), Chongqing, China, 11–13 October 2019; pp. 1636–1642.

8. Wei, J.; Cao, S. Application of Edge Intelligent Computing in Satellite Internet of Things. In Proceedings of the 2019 IEEE International Conference on Smart Internet of Things (SmartIoT), Tianjin, China, 9–11 August 2019; pp. 85–91.
9. Xu, D.; Zhang, G.; Ding, X. Analysis of Co-channel Interference in Low-orbit Satellite Internet of Things. In Proceedings of the 2019 15th International Wireless Communications & Mobile Computing Conference (IWCMC), Tangier, Morocco, 24–28 June 2019; pp. 136–139.
10. Qu, Z.; Zhang, G.; Cao, H.; Xie, J. LEO Satellite Constellation for Internet of Things. *IEEE Access* **2017**, *5*, 18391–18401. [CrossRef]
11. Kak, A.; Guven, E.; Ergin, U.E.; Akyildiz, I.F. Performance Evaluation of SDN-Based Internet of Space Things. In Proceedings of the 2018 IEEE Globecom Workshops (GC Wkshps), Abu Dhabi, United Arab Emirates, 9–13 December 2018; pp. 1–6.
12. Zhang, Z.; Li, Y.; Huang, C.; Guo, Q.; Liu, L.; Yuen, C.; Guan, Y.L. User Activity Detection and Channel Estimation for Grant-Free Random Access in LEO Satellite-Enabled Internet of Things. *IEEE Internet Things J.* **2020**, *7*, 8811–8825. [CrossRef]
13. Routray, S.K.; Tengshe, R.; Javali, A.; Sarkar, S.; Sharma, L.; Ghosh, A.D. Satellite Based IoT for Mission Critical Applications. In Proceedings of the 2019 International Conference on Data Science and Communication (IconDSC), Bangalore, India, 1–2 March 2019; pp. 1–6.
14. Dwivedi, A.K.; Chokkarapu, S.P.; Chaudhari, S.; Varshney, N. Performance Analysis of Novel Direct Access Schemes for LEO Satellites Based IoT Network. In Proceedings of the 2020 IEEE 31st Annual International Symposium on Personal, Indoor and Mobile Radio Communications, London, UK, 31 August–3 September 2020; pp. 1–6.
15. Zhang, X. *Study on Modeling and Simulation of the Meteorological Satellite Channel under Different Weather Conditions*; Nanjing University of Information Engineering: Nanjing, China, 2014.
16. Jian-fei, Z.; Guang, D.; Jian-Dong, Y.; Xiao-Yun, T. Influence of Ocean Clouds and Precipitation to Shipborne High Frequency Band Satellite Communication. *J. Electron.* **2018**, *46*, 381–386. [CrossRef]
17. Li, J.; Fong, S.; Zhuang, Y. Optimizing SMOTE by Metaheuristics with Neural Network and Decision Tree. In Proceedings of the 2015 3rd International Symposium on Computational and Business Intelligence (ISCBI), Washington, DC, USA, 7–9 December 2015; pp. 26–32. [CrossRef]
18. Ma, W. SMOTE-based Category Imbalance for Radar Radiation Source Sorting and Identification. In Proceedings of the 2020 IEEE International Conference on Information Technology, Big Data and Artificial Intelligence (ICIBA), Chongqing, China, 6–8 November 2020; pp. 1291–1294. [CrossRef]
19. Chen, L.; Dong, P.; Su, W.; Zhang, Y. Improving Classification of Imbalanced Datasets Based on KM++ SMOTE Algorithm. In Proceedings of the 2019 2nd International Conference on Safety Produce Informatization (IICSPI), Chongqing, China, 28–30 November 2019; pp. 300–306. [CrossRef]
20. Wang, M.; Cui, X.; Yu, B.; Chen, C.; Ma, Q.; Zhou, H. SulSite-GTB: Identification of protein S-sulfenylation sites by fusing multiple feature information and gradient tree boosting. *Neural Comput. Appl.* **2020**, *32*, 13843–13862. [CrossRef]
21. Zehai, G.; Cunbao, M.; Jianfeng, Z.; Weijun, X. Remaining useful life prediction of integrated modular avionics using ensemble enhanced online sequential parallel extreme learning machine. *Int. J. Mach. Learn. Cybern.* **2021**, *12*, 1893–1911. [CrossRef]
22. Sun, P.; Liu, P.; Li, Q.; Liu, C.; Lu, X.; Hao, R.; Chen, J. DL-IDS: Extracting Features Using CNN-LSTM Hybrid Network for Intrusion Detection System. *Secur. Commun. Netw.* **2020**, 2020. [CrossRef]
23. Liu, W.; Chen, X.; Sun, M.; Mei, C.; Li, Y.; Qi, M.; Gao, H. Multivariate Load Interval Prediction of Integrated Energy System Based on Multitask Learning. In Proceedings of the 2019 IEEE Sustainable Power and Energy Conference (iSPEC), Beijing, China, 20–24 November 2019.